



SUBJECT: MGT – Trip Report – Geophysical Assistance

9 June 2015

TO: Gregory A. Kist
State Conservationist, NRCS
441 S Salina Street, RM 520
Syracuse, NY 13202-2450

File Code: 330-20-7

Purpose:

To provide geophysical field assistance to several engineering projects in Chautauqua and Genesee Counties, New York. Ground-penetrating radar (GPR) and electromagnetic induction (EMI) were used to assess the structural integrity of the earthen dam structure in Chautauqua County, and the presence of geologic hazards beneath two proposed waste-storage sites located in areas of karst in Genesee County.

Participants:

Rachel Arnold, Student Intern, USDA-NRCS, Batavia, NY
Bob Bills, Resource Conservationist, USDA-NRCS, Albion, NY
Scott Contractor, Operator, Alleghany Farm Services, Basom, NY
Randy Dibble, Operator, Alleghany Farm Services, Basom, NY
Jim Doolittle, Research Soil Scientist, USDA-NRCS-NSSC, Newtown Square, PA
Heath Eisele, District Conservationist, USDA-NRCS, Batavia, NY
Jarred Elliott, Technician, Genesee County SWCD, Batavia, NY
Jim Guistina, Engineer, Ty Lynn International,
Chris Hall, Student Intern, USDA-NRCS, Geneseo, NY
Marie Hauser, Engineer, TY Lynn International,
Chris Henry, Civil Engineer, USDA-NRCS, Syracuse, NY
Li Kui, Student Intern, USDA-NRCS, Batavia, NY
Steve Perschke, West Area Engineer, USDA-NRCS, Batavia, NY
Paul Richards, Professor, SUNY Brockport, NY
Drew Rogers, Engineer, Chautauqua County Public Works, Little Valley, NY
Bob Shenk, Technician, Cattaraugus County Soil & Water Conservation District, Ellicottville, NY
Steven Sprecher, Soil Scientist, USDA-NRCS, Geneseo, NY
George Squires, Manager, Genesee County SWCD, Batavia, NY
Molly Stetz, Technician, Genesee County SWCD, Batavia, NY
Olga Vargas, Resource Soil Scientists, USDA-NRCS, Greenwich, NY

Activities:

All geophysical surveys were completed on 19 to 20 May 2015.

Summary:

1. Most earthen dam structure are composed of fine- and medium-textured earthen materials, which are highly attenuating and therefore depth restrictive to ground-penetrating radar. For the investigation of the Conewango Watershed flood control dam, a 70 MHz antenna was used. This is the lowest frequency and provides the greatest exploration depth of all antennas operated by USDA. High rates of signal attenuation resulted in depth-restrictive (<2 m) radar data, which was

of limited value to investigators. Based on these results, future use of GPR for the investigation of dams should be restricted to concrete structures and those composed of relatively coarse textured materials.

2. At the Conewango Watershed flood control dam, EMI provided detailed information on spatial variations in EC_a , which were associated with differences in moisture and clay contents. Results obtained with an EM31 meter, while suggesting variations in moisture contents, did not reveal any major physical deficiency or weakness passing through the structure. However, while generally conforming to predictable patterns, slight intrusions of higher EC_a were observed extending in an upslope direction along the base of the dam. Though seemingly slight and insignificant, these areas may indicate seepage and excess water, and warrant further attention.
3. At each of the three sites surveyed with the EMP-400 Profiler, EC_a data collected at different frequencies were highly correlated. Although the relative response at different frequencies varied in amplitude, spatial patterns and interpretations were similar. The high correlation among the data sets and resulting similar spatial EC_a patterns suggest that multiple depths and additional subsurface information are not being attained with multifrequency Profiler.
4. At the Post Farm site, spatial EC_a patterns provided evidence of anomalous subsurface conditions, but these patterns cannot be unambiguously associated with solution features. In retrospect, a larger survey area may have provided better definition and improved insight into the anomalies detected with EMI. Soil borings and cores are required to confirm EMI interpretations and the presence of solution features.
5. Results of GPR surveys indicates a consistently thick clay liner (average of 0.73 m) and relatively uniform depth to limestone bedrock beneath a recently excavated waste-holding pit at the Offhaus Farms. High resolution GPR surveys indicate the presence of layering and minor fractures or solution features within the upper portion of the underlying limestone bedrock. Results of EMI surveys conducted with the Profiler do not indicate the presence of major solution features. Though unconfirmed, results do indicate a major change in the underlying lithology and possibly high levels of magnetic susceptibility caused by the concentrations of iron oxides.
6. Results of geophysical investigations are interpretive and do not substitute for direct ground-truth observations (core samples obtained by drilling). Geophysical methods do permit the visualization of some subsurface trends and localized anomalous conditions that can be missed by all but the most close-spaced drilling programs. The use of geophysical methods can reduce the number of cores, direct their placement, and supplement their interpretations.
7. Between May 1984 and May 2015, Jim Doolittle participated in 49 field assistance projects in New York. Jim is deeply grateful to the SCS and NRCS personnel who worked with and assisted him on these projects. Knowledge has been gained from these investigations and several papers written documenting these experiences. This is Jim's last trip as a NRCS employee to New York. He wishes you and your staff "Fair Winds and Following Seas."

It was the pleasure of Jim Doolittle and the National Soil Survey Center to work in New York and to be of assistance to you and your staff.

JONATHAN W. HEMPEL
Director
National Soil Survey Center

Attachment (Technical Report)

cc:

James Doolittle, Research Soil Scientist, Soil Survey Research & Laboratory, NSSC, MS 41, USDA-NRCS, Newtown Square, PA

Luis Hernandez, Soil Survey Regional Director, Glaciated Soil Survey Region (SSR 12), USDA-NRCS, Amherst, MA

Chris Henry, Civil Engineer, USDA-NRCS, Syracuse, NY

Steve Perschke, West Area Engineer, USDA-NRCS, Batavia, NY

Richard Shaw, State Soil Scientist, USDA-NRCS 220 Davidson Ave., 4th Floor, Somerset, NJ
08873-4115

Wes Tuttle, Soil Scientist (Geophysical), USDA-NRCS-NSSC, Wilkesboro, NC

Daniel Vellone, Geologist, USDA-NRCS, Holden, MA

Michael Wilson, Research Soil Scientist/Liaison MO12, Soil Survey Research & Laboratory, NSSC, MS 41, USDA-NRCS, Lincoln, NE

Douglas Wysocki, National Leader, Soil Survey Research & Laboratory, NSSC, MS 41, NRCS, Lincoln, NE

Technical Report

James A. Doolittle

Background:

The use of geophysical methods can permit the visualization of some structural trends and localized anomalous conditions in earthen structures, which are often overlooked by all but the most closely-spaced drilling programs (Butler and Llopis, 1990). Butler and Llopis (1990) considered electromagnetic induction (EMI) and ground-penetrating radar (GPR) as the primary and secondary geophysical tools, respectively, for the detection of anomalous zones and areas of seepage in earthen structures. Ground-penetrating radar is suited to shallow (generally less than 5 to 10 meters) profiling of earthen materials that have low clay and salt contents. Compared with other geophysical methods, GPR can provide the highest resolution of subsurface features. Ground-penetrating radar has been used to locate voids and buried pipes (Karastathis *et al.*, 2002), and to monitor deterioration processes in some concrete dams (Rhim, 2001). In addition, GPR has been used to locate voids and characterize internal structures in coarse-textured embankment materials used in dams with concrete (Silver *et al.*, 1986) or clay (Dominic *et al.*, 1995) cores. Because of its dependency on soil properties, the appropriateness of GPR for the investigations of earthen structures is highly variable. Because dam structures are typically composed of finer-textured soil materials, which are more attenuating to propagated radar energy, most results have been depth-restrictive and of limited value.

Advantages of EMI are its portability, speed of operation, flexible observation depths, and moderate resolution of subsurface features. Electromagnetic induction uses electromagnetic energy to measure the apparent conductivity (EC_a) of earthen materials. Apparent conductivity is the weighted, average conductivity for a column of earthen materials (Greenhouse and Slaine, 1983). Variations in EC_a are produced by differences in the electrical conductivity of earthen materials. Electrical conductivity is principally influenced by volumetric water content, type and concentration of ions in solution, temperature and phase of the soil water, and amount and type of clays in the soil matrix (McNeill, 1980a). The EC_a of earthen materials increases with increased soluble salt, water, and clay contents (Kachanoski *et al.*, 1988; Rhoades *et al.*, 1976).

The resolution of EMI is inferior to that obtained with electrically resistivity and GPR. In addition, as with all geophysical methods, the resolution of subsurface features decreases with increasing exploration depths. As a result, the detection of anomalous features within and below earthen structures with EMI depends on the size, depth, and composition (contrasting materials) of these features.

Electromagnetic induction techniques have been used in areas of karst (Canace and Dalton, 1984; Pazuniak, 1989; Robinson-Poteet, 1989; Rumbens, 1990). In these studies, interpretations of EMI data enabled the delineation of larger subsurface voids, channels, and zones of higher permeability (such as fractures and karstified areas within carbonate bedrock). Typically, the shape and pattern of the subsurface anomaly have been used to identify the solution feature.

Survey Sites:

Conewango Watershed Site 3, Flood Control Dam:

Conewango Watershed Site 3 (42.2508 ° N latitude, 79.1734 ° W longitude) is located off of Edson Road (CR 617), about 4.0 miles northwest of Ellington, New York. Fig 1 is a soil map of the structure's site from the Web Soil Survey.¹ Principal soils mapped in the area surrounding the dam include different

¹ Soil Survey Staff, Natural Resources Conservation Service, United States Department of Agriculture. Web Soil Survey. Available online at <http://websoilsurvey.nrcs.usda.gov/>. Accessed [05/27/2015].

phases of Chadakoin (coarse-loamy, mixed, superactive, mesic Typic Dystrudepts), Chautauqua (coarse-loamy, mixed, active, mesic Aquic Dystrudepts), and Valois (coarse-loamy, mixed, superactive, mesic Typic Dystrudepts) soils. These very deep and deep, moderately well drained and well drained soils formed in till derived from sandstone, siltstone and shale, and have moderate potential for GPR applications.



Figure 1. This soil map of the Conewango Watershed Dam site is from the Web Soil Survey. Principal soils in the area surrounding the dam include different phases of Chadakoin (ChD, ChE), Chautauqua (CkB, CkC), and Valois (VaD, VaF) soils.

Post Farm site:

The Post Farm site (43.04778° N latitude, 78.2089° W longitude) is located just north of the Batavia-Elba Township Road, and about 3.5 miles north-northwest of the center of Batavia, New York. Figure 2 is a soil map of the study site showing the primary waste-holding facility, which was drained and scrapped clean before the EMI survey². The waste-holding facility will be expanded to the north and northwest of the existing structure, and into areas mapped as Ovid (fine-loamy, mixed, active, mesic Aeric Endoaqualfs) and Cazenovia (fine-loamy, mixed, active, mesic Oxyaquic Hapludalfs) soils. The very deep, somewhat poorly drained Ovid and the moderately well drained Cazenovia soils formed in moderately-fine textured till. These soils have moderate potential for GPR investigations. At this site, EMI surveys were completed on the base of the existing waste-holding structure and across the area of the planned expansion.

Offhaus Farm site:

The Offhaus Farm site (43.0322 ° N latitude, 78.2085 ° W longitude) is located off of Oak Orchard Road (NY 98), and about 2.5 north-northwest of the center of Batavia New York. Figure 3 is a soil map of the study area from the Web Soil Survey.² The site is located in a field of Ontario silt loam, 3 to 8 percent slopes. The very deep, well drained Ontario (fine-loamy, mixed, active, mesic Glossic Hapludalfs) soils

² Soil Survey Staff, Natural Resources Conservation Service, United States Department of Agriculture. Web Soil Survey. Available online at <http://websoilsurvey.nrcs.usda.gov/>. Accessed [05/27/2015].

formed in till that is strongly influenced by limestone. The newly completed waste-holding facility has been excavated to limestone bedrock and covered with a 2 foot “clay” liner. The Ontario soil has moderate potential for GPR investigations. Both GPR and EMI surveys were completed on the base of the newly excavated waste-holding facility.

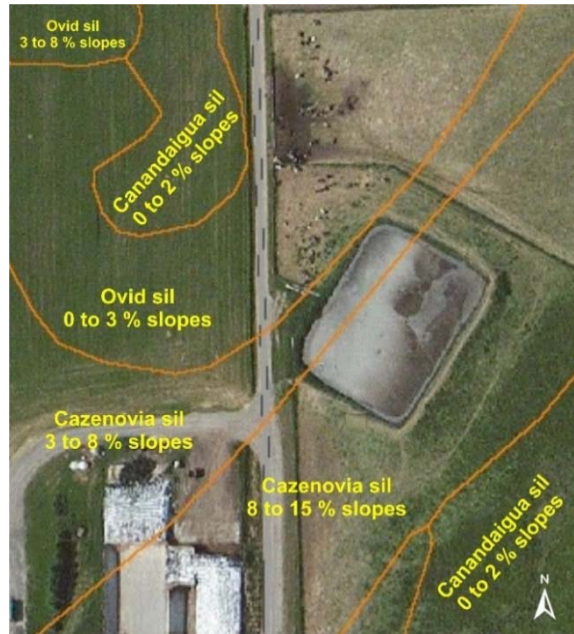


Figure 2. This soil map of the Post Farm site is from the Web Soil Survey. The existing waste-holding structure will be expanded to the north and northwest and into the area to the immediate east of the farm road.



Figure 3. This soil map of Offhaus Farm site is from the Web Soil Survey. The rectangle identifies the approximate location of the recently excavated waste-holding facility that was surveyed with EMI and GPR.

Equipment:

The radar unit is the TerraSIRch Subsurface Interface Radar (SIR) System-3000, manufactured by Geophysical Survey Systems, Inc. (GSSI; Nashua, NH).³ The SIR-3000 system consists of a digital control unit (DC-3000) with keypad, SVGA video screen, and connector panel. A 10.8-volt lithium-ion, rechargeable battery powers the system. The SIR-3000 weighs about 4.1 kg (9 lbs.) and is backpack portable. With an antenna, the SIR-3000 system requires two people to operate. Operating procedures for the SIR-3000 are described by Geophysical Survey Systems, Inc. (2004). Jol (2009) and Daniels (2004) discuss the use of GPR. Three antennas (70, 120, and 400 mHz) were used in this study. The 70 mHz antenna is the lowest frequency antenna available to USDA-NRCS. Lower frequency antennas provide greater penetration depths than higher frequency antennas. The RADAN for Windows (version 7.0) software program (developed by GSSI) was used to process and to improve the recognition of radar reflection pattern appearing on radar records.³

The SIR-3000 system has a setup for the use of a GPS receiver with a serial data recorder. With this setup, each scan on radar records can be georeferenced (position/time matched). During data processing, a subprogram within RADAN is used to proportionally adjust the position of each radar scan according to the time stamp of the two nearest positions recorded with the GPS receiver. A Trimble AG114 GPS receiver (Trimble, Sunnyvale, CA) was used to georeferenced the GPR data collected at the Offhaus Farm³. Position data were recorded at a rate of one reading per second.

Two EMI sensors were used in this study: the Profiler EMP-400 and the EM31 meter. The Profiler EMP-400 is a multifrequency EMI meter that can simultaneously collect data in as many as three discrete frequencies. For each frequency, in-phase, quadrature phase, and conductivity data are recorded. The Profiler EMP-400 sensor (here after referred to as the Profiler) is manufactured by Geophysical Survey Systems, Inc. (Nashua, NH)³. Operating procedures for the Profiler are described by Geophysical Survey Systems, Inc. (2008). The Profiler weighs about 4.5 kg, (9.9 lbs.) and has a 1.2 m (4.0 ft) intercoil spacing. It operates at frequencies ranging from 1 to 16 kHz, which are selectable in 1-kHz steps. The calibration of the Profiler is optimized for 15 kHz and, as a consequence, EC_a is most accurately measured at this frequency (Dan Delea, GSSI, personal communication).

Surveys were conducted with the Profiler held in the deeper-sensing, vertical dipole orientation (VDO). Data were recorded at 15000, 10000, and 5000 Hz. The sensor's electronics are controlled via Bluetooth communications with a Trimble Tripod Data System RECON-400 Personal Data Assistant (PDA) and its application software³. The PDA has an integrated Bluetooth service and Holux™ Wide Area Augmentation System Global Position System (WAAS-GPS) with differential correction horizontal dilution of precision (HDOP)³. All EC_a acquisition points were georeferenced and used to construct the plots shown in this report.

The EM31 meter is manufactured by Geonics Limited³. It weighs about 12.4 kg (27.3 lbs.), has a 3.66 m intercoil spacing, and operates at a frequency of 9,810 Hz. When placed on the soil surface, the EM31 meter has effective depths of exploration of about 0 to 6 meters in the VDO (McNeill, 1980b). McNeill (1980b) has described the principles of operation for the EM31 meter.

A Trimble AG114 GPS receiver was used to georeferenced EMI data collected with the EM31 meter. Position data were recorded at a rate of two reading per second. The Geonics DAS70 Data Acquisition System was used with the EM31 meter to record and store both EC_a and GPS data. The acquisition system consists of an EMI meter, GPS receiver, and an Allegro CX field computer (Juniper Systems, Logan, Utah).³ The RTmap31 software program developed by Geomar Software Inc. (Mississauga,

³ Manufacturer's names are provided for specific information; use does not constitute endorsement.

Ontario) was used with the EM31 meter and the Allegro CX field computer to record, store, and process EC_a and GPS data⁴. Figure 4 shows the survey of Conewango Flood Control Dam being conducted with the EM31 meter, Allegro CX field computer (in left hand), and AG114 GPS (in backpack).

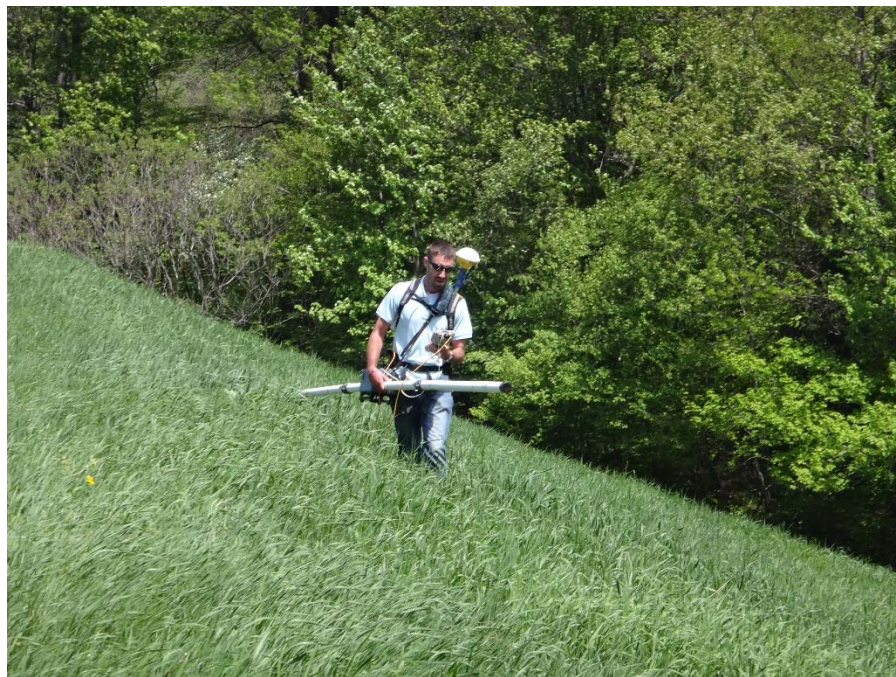


Figure 4. Chris Lee conducts an EMI survey with the EM31 meter across the steep face of the Conewango earthen dam structure.

Both EMI sensors need only one person to operate and require no ground contact (Figure 4). Lateral resolution is approximately equal to the intercoil spacing of the instruments. To help summarize the results of the EMI survey, SURFER for Windows (version 10.0) software (Golden Software, Inc., Golden, CO) was used to construct the simulations shown in this report⁴. Plots of EMI data shown in this report were created using kriging methods with an octant search.

Depth of Exploration:

As knowledge of the effective depth of exploration (d_e) is essential for the proper interpretation of EMI data, a brief discussion of this parameter is presented. The depth of exploration can be defined as “the maximum depth at which a given target in a given host can be detected by a given sensor” (Huang, 2005). The d_e depends on both the coil offset (intercoil spacing) and the frequency, and can be increased by either increasing the intercoil spacing or by decreasing the frequency.

McNeill (1980b) noted that the d_e for the EM31 meter is *geometry limited* and dependent on coil separation, coil orientation, and frequency. Larger coil separations and lower frequencies are used to achieve greater d_e , but have lower signal amplitude than meters with shorter coil separations and higher frequencies. When operated under conditions of *low induction number* (LIN), the depth-response of the EM31 meter is assumed to be independent of soil conductivity. Conditions of low induction number are assumed to be satisfied in soils that have low (<100 mS/m) EC_a (McNeill, 1980b). However, some believe that McNeill's LIN approximations uses restrictive physical and mathematical assumptions to derive a solution and are therefore valid only in some soil settings (Callegary *et al.*, 2007). Results of numerical simulations conducted by Callegary *et al.* (2007) indicate that the spatial sensitivity and d_e of

⁴ Manufacturer's names are provided for specific information; use does not constitute endorsement.

LIN sensors varies significantly with changes in bulk electrical conductivity. Greenhouse *et al.* (1998) earlier noted that the electrical conductivity of soils plays a critical role in the d_e obtained with all EMI sensors. Slavich (1990) and de Jong *et al.* (1979) also reported that the d_e varies depending on the bulk electrical conductivity of the profiled material(s). Callegary *et al.* (2007) cautioned that only in most electrically resistive soils are the LIN approximations and its predictions of d_e correct.

Won *et al.* (1996) observed that for multifrequency sensors, such as the Profiler, changing the transmitter frequency will change the d_e . In theory, lower frequencies provide greater d_e . Won (1980 and 1983) maintains that the d_e of multi-frequency EMI sensors is governed by the *skin-depth effect*: lower frequency signals travel farther through conductive mediums than higher frequency signals. The *skin effect* is the tendency for electrical current density to be greatest at the surface and decreases exponentially with depth. Skin depth represents the maximum d_e for the Profiler operating at a given frequency and sounding a medium of known conductivity. Theoretically, the maximum d_e or skin depth is inversely proportional to frequency (Won *et al.*, 1996). Low frequency signals have longer periods of oscillation, loose energy less rapidly, and achieve greater d_e than high frequency signals. In addition, for a given frequency, the d_e is greater in low than in high conductivity soils. Huang (2005) calculated that the d_e is approximately equal to the square root of the skin depth. In addition, Huang (2005) noted that for a given skin depth, the depth of exploration increases with the target conductivity and conductivity contrast.

Multifrequency EMI sensors continue to challenge users. McNeill (1996) contends that multiple frequencies EMI sensors do not offer any advantages over single-frequency sensors. Brosten *et al.* (2011), using synthetic modeling methods, determined that a GEM-2 multifrequency sensor (similar to the Profiler), in a medium with an estimated skin depth of 23.4 m (76.8 ft), had an actual d_e that ranged from only 1.8 to 2.7 m (5.9 to 8.9 ft). Based on the findings of Brosten *et al.* (2011), the Profiler is viewed by this observer as a geometry limited sensor, like the EM31 meter. Assuming LIN conditions, the effective exploration depths of the Profiler (when placed on the ground surface and operated in the VDO) is assumed to be approximately 1.8 m (5.9 ft) as opposed to 6 m (19.7 ft) for the EM31 meter.

Calibration of GPR:

Ground-penetrating radar is a time scaled system. The system measures the time that it takes electromagnetic energy to travel from an antenna to an interface (e.g., bedrock, soil horizon, stratigraphic layer) and back. To convert the two-way travel time into a depth scale, either the velocity of pulse propagation or the depth to a reflector must be known. The relationships among depth (D), two-way pulse travel time (T), and velocity of propagation (v) are described in equation [1] (after Daniels, 2004):

$$v = 2D/T \quad [1]$$

The velocity of propagation is principally affected by the relative dielectric permittivity (E_r) of the profiled material(s) according to equation [2] (after Daniels, 2004):

$$E_r = (C/v)^2 \quad [2]$$

In equation [2], C is the speed of light in a vacuum in a vacuum (0.3 m/ns). Typically, the velocity of pulse propagation is expressed in meters per nanosecond (ns). In soils, the amount and physical state (temperature dependent) of water have the greatest effect on the E_r and v .

At the Offhaus Farm site, based on the measured depth and the two-way pulse travel time to limestone bedrock, the average velocity of propagations and the relative dielectric permittivity through the upper part of the Amenia soil profile was estimated using equations [1] and [2]. The estimated E_r was 5.97. The estimated v was 0.1228 m/ns. At the Conewango Watershed site, hyperbola velocity analysis was

used to determine the E_r and v . Hyperbola velocity analysis involves matching an ideal form of a velocity-specified hyperbolic function to the form appearing on the radar record. Cassidy (2009) reported that hyperbolic matching methods produce estimated velocity values with error and variance of $\pm 10\%$ or more. Based hyperbola matching, the average E_r was estimated to be 13.0, which corresponds to an average v of 0.0832 m/ns.

Results:

Conewango Watershed Site 3, Flood Control Dam

Ground-penetrating radar traverse were conducted along the top of the centerline of the embankment with a 70 MHz antenna. Pulses of electromagnetic energy transmitted into the soil from this antenna are less rapidly attenuated and should achieve greater d_e than with other antennas operated by NRCS. Unfortunately, even with the 70 MHz antenna, earthen embankment materials provide an unfavorable setting for deep investigations with GPR. Here, GPR profiling was restricted to depths of less than 2 meters (see figure 5). In addition, levels of background noise were exceptionally high and, even after significant signal processing, the reflection patterns appearing on radar records were difficult to satisfactorily image because of the low signal to noise ratio. On the radar record shown in Figure 5, a segmented white-colored line has been used to highlight a subsurface interface. This boundary varies in depth from 1.45 to 2.01 m. With the exception of this interface, no other subsurface feature can be identified. In the central portion of this radar record, a zone of exceptionally high-amplitude reflections represents background noise that was not removed by signal processing. The numerous “point reflectors” that appear in horizontal bands in the lower part of this radar record represent background noise caused by the up-and-down movement and jarring of the antenna. Even with low frequency antennas, the use of GPR for the investigation of earthen embankments is depth restrictive and provides limited subsurface information.

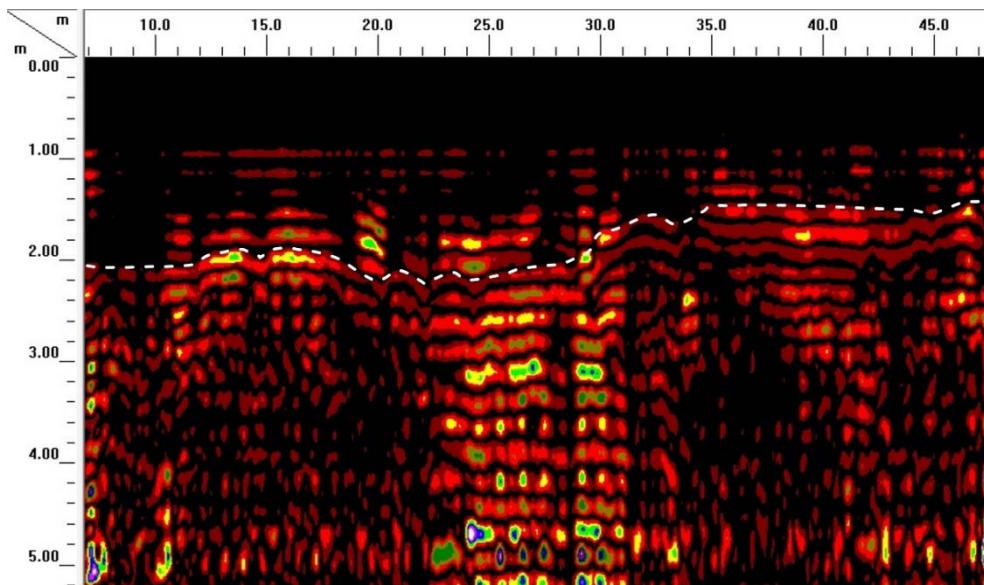


Figure 5. This processed radar record was collected with a 70 MHz antenna along the centerline of the Conewango Watershed Flood Control Dam. All scales are expressed in meters. A subsurface interface is identified by the white-colored segment line.

Detailed EMI surveys were conducted across the earthen structure with both the EM31 meter and the Profiler. Based on 1675 EC_a measurements made with the EM31 meter, EC_a averaged 12.87 mS/m, and ranged from 9.0 to 23.8 mS/m across this site. However, one-half of the recorded measurements were between values of only 11.5 and 14.0 mS/m. These values are considered representative of moist, loamy materials.

Figure 6 is a two-dimensional plot of the Conewango Watershed flood control structure showing the spatial variation in the EC_a measured with the EM31 meter. In this plot, a black-colored segmented line has been used to identify the center line of the structure. Values of EC_a are lowest along the crest of the structure and are highest along the lower side slopes and base of the structure. This trend is attributed to increased soil moisture contents along the lower slopes of the dam. There is some suggestion of layering across the structure. Layers appear to generally parallel the contours of the earthen dam structure and reflect variations in clay and moisture contents. However, exceptions are evident in the irregularity of isolines with zones of higher and lower EC_a extending upwards and downwards across portions of this structure. In Figure 6, the anomalously high EC_a near “A” is believed to reflect metallic features in a pipe or conduit leading from a nearby concrete riser through the dam structure.

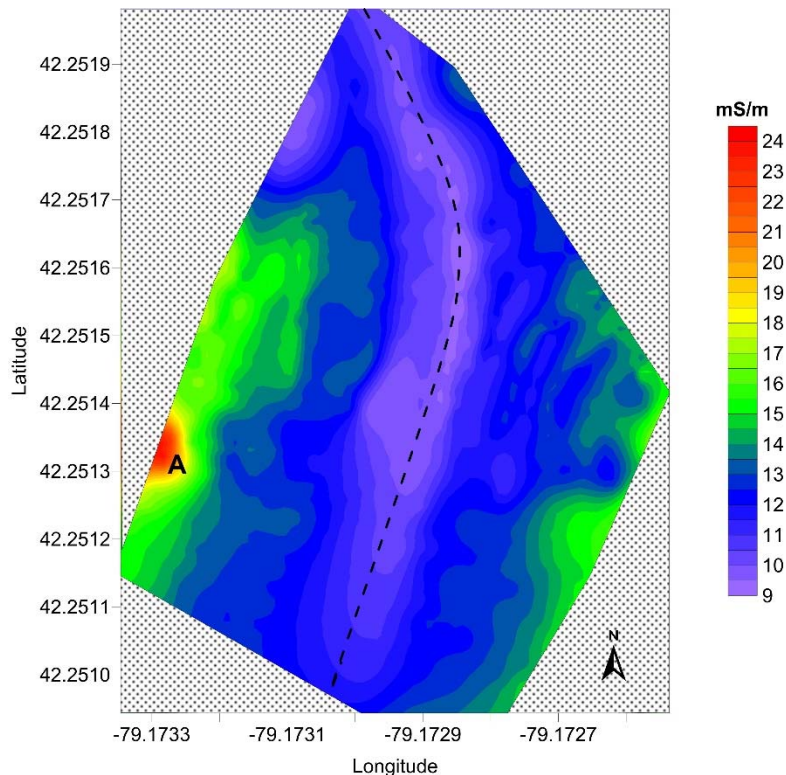


Figure 6. A two-dimensional plot of the EC_a data measured with the EM31 meter across the Conewango Flood Control Dam.

Figure 7 is a three-dimensional (3D) wireframe image of the Conewango Watershed flood control structure with the EC_a data draped over it. Because of the lower vertical accuracy of GPS, the recorded elevation data provide a general though not precise portrayal of the topography of this site (with all GPS receivers, vertical accuracy (elevation) is generally lower than horizontal accuracy). Again, the lowest EC_a is recorded along the centerline of the structure (see “A” in Figure 7) where soils are better drained and have presumably lower moisture contents. While generally conforming to predictable patterns, slight intrusions in an upslope direction of areas of higher EC_a can be observed (see “B” in Figure 7). Though seemingly slight and insignificant, these areas may indicate seepage and excess water, and warrant further inspection or monitoring. On this 3D image, a noticeable linear pattern of lower EC_a that extends in an upslope direction is evident at “C”. With slight resourcefulness, a linear pattern of lower EC_a can be extended across and connected with the concrete riser along the western base of the structure (see white-colored segmented line in Figure 7). It is believed that this faint lineation of low EC_a represents the concrete conduit that passes through the structure.

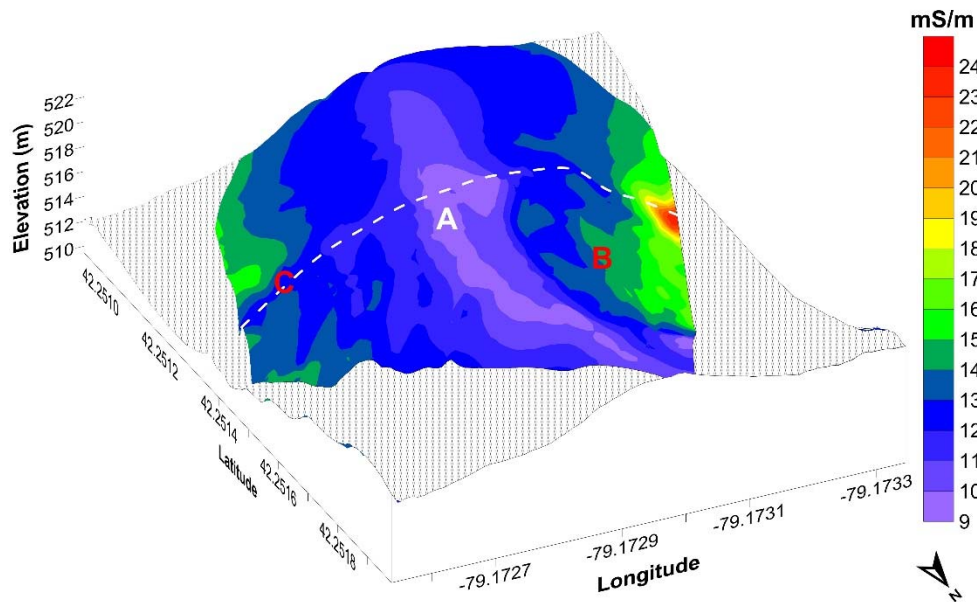


Figure 7. A three-dimensional plot of the EC_a data measured with the EM31 meter across the Conewango Watershed flood control dam.

Figure 8 contains plots of EMI data that were measured at the Conewango Watershed flood control structure with the Profiler. In Figure 8, the upper, middle, and lower plots show spatial EC_a data recorded at 15000, 10000 and 5000 Hz, respectively. As evident in Figure 8, a large portion of the earthen dam structure, which was surveyed with the EM31 meter (see figure 6), was not surveyed with the Profiler. This was unfortunate as it limited the area of comparison for the two EMI sensors.

As evident in Figure 8, EC_a increases with increasing frequency and decreasing depth of exploration. Based on 2067 measurements, EC_a averaged 22.9, 19.8, and 14.0 mS/m at frequencies of 15, 10 and 5 kHz, respectively. Apparent conductivity measured at 15 kHz ranged from -10.4 to 33.6 mS/m, with 95% of the measurements occurring between 17.9 and 28.9 mS/m. At 10 kHz, EC_a ranged from -39.1 to 32.1 mS/m, with 95% of the measurements occurring between 15.0 and 25.0 mS/m. At 5 kHz, EC_a ranged from -136.0 to 49.3 mS/m, with 95% of the measurements occurring between 7.4 and 20.0 mS/m. The large ranges in EC_a are attributed to metallic artifacts scattered across the site and random noise. During recording, signal averaging by stacking can improve the signal-to-noise ratio and reduce random noise. Stacking is automatically set on the Profiler according to the number of frequencies selected and the rate of recording specified. Decreasing the number of frequencies recorded or increasing the sampling interval will allow higher levels of stacking.

In Figure 8, the EC_a data collected with the Profiler do not appear to reflect the increase on lower slope components that was detected with the EM31 meter. With the Profiler, EC_a decreases with increasing soil depth (lower frequency). The spatial EC_a patterns have a noticeable, band-like appearance with overall amplitudes increasing with increasing frequency (shallower d_e). These bands could reflect difference in texture and moisture contents within the structure. However, adjoining bands have alternating, repetitive sequences of higher and lower amplitudes suggesting some form of noise. In addition, isolated point anomalies are more apparent at lower frequencies. The bands and point anomalies evident in the Profiler data may reflect differences in physical properties, but are suspected to represent background noise. In addition, the repeatability and accuracy of EC_a measurements are influenced by the tilt and height of the

sensor above the ground and may vary along and among the line traverse lines especially in areas of steeply sloping terrains such as the embankment. Lower frequencies are more sensitive to tilting errors. At this site, it is difficult to maintain a constant sensor height due to the non-smoothness of the micro-topography, the general steep slope of the embankment, and the present of vegetation. These factors may have contributed to the banding that is apparent in Figure 8.

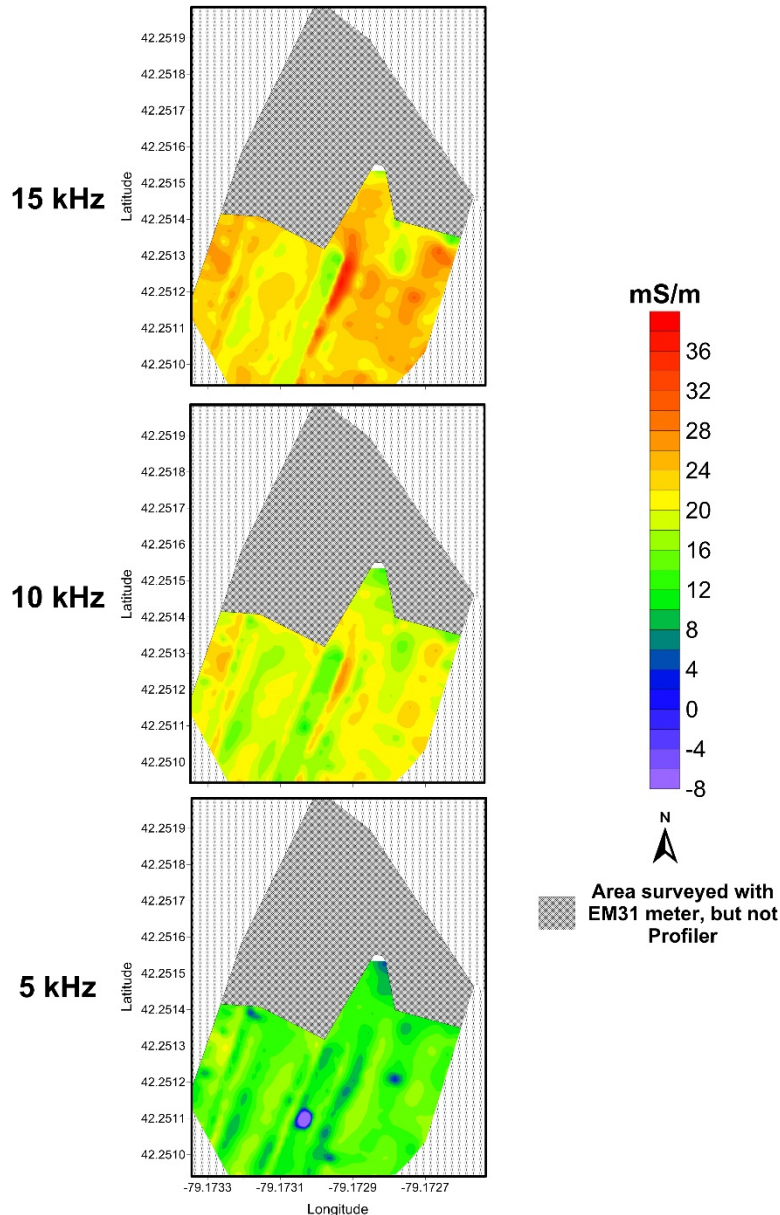


Figure 8. These three, two-dimensional plot of the EC_a data were measured with the Profiler sensor at frequencies of 15 (upper plot), 10 (middle plot), and 5 (lower plot) Hz across a portion of the Conewango Watershed flood control dam.

As evident in Figure 8, the collection of EMI data at different frequencies with the Profiler appears to result in similar EC_a spatial pattern and interpretations. Table 1 shows the correlation among the EC_a measurements made at the different frequencies. Electrical conductivity values derived from adjacent frequencies are highly correlated with each other. As evident in Table 1, the closer the frequencies (i.e.

15 and 10 kHz, and 10 and 5 kHz) the higher the correlation. The correlations shown in Table 1 and the similarity of spatial patterns evident in the three plots of Figure 8 (except in response amplitudes), suggest that the use of multiple frequencies provides similar and redundant information.

Table 1. Correlations among data sets recorded at different frequencies with the Profiler.

	15 kHz	10 kHz	5 kHz
15 kHz	1.0000	0.8030	0.5598
10 kHz	0.8030	1.0000	0.8521
5 kHz	0.5598	0.8521	1.0000

At the Conewango Watershed flood control structure, the EM31 meter appears to provide deeper, more consistent and useful information than the Profiler.

Post Farms:

Separate surveys were conducted with each EMI sensor across both (1) the base of the emptied animal-waste storage pit and (2) the planned storage pit expansion area to the immediate northwest and north of the existing structure. In the proposed expansion area, based on 535 EC_a measurements made with the EM31 meter, EC_a averaged 14.9 mS/m, with values ranging from 8.6 to 26.6 mS/m. In the emptied waste pit, based on 932 EC_a measurements made with the EM31 meter, EC_a averaged 16.2 mS/m, with values ranging from 11.4 to 30.0 mS/m. The floor of the emptied waste pit was at a lower elevation (about 3 m) than the surface of the expansion area, and, as a consequence, the EM31 meter profiled different and deeper strata. The slightly higher EC_a measured along the base of the emptied pit is associated with higher soluble salt contents from residual animal waste products in the underlying materials. In general, EC_a values measured with the EM31 meter were low and representative of medium textured materials formed in till.

Figure 9 contains plots showing spatial variations in the EC_a data that were measured with the EM31 meter across (A) the planned storage pit expansion area to the immediate northwest and north of the existing structure, and (B) the base of the emptied animal-waste storage pit. In the expansion area, two soil pits were excavated to depths of about 2 m to confirm interpretations (see red-colored point symbols in Figure 9A). Higher and lower EC_a recorded at these sites were directly related to variations in clay contents; the western pit had slightly higher clay contents than the eastern pit. Based on these findings, the spatial patterns shown on these plots are assumed to principally reflect variations in sediment texture and moisture contents.

As the expansion area and existing pit are in an area of karst, the large circular area of higher EC_a in the northwest corner of Figure 9A could be suspected of representing a larger solution cavity, which is filled with medium-textured soil materials. A thicker clay column and greater depth to more electrically resistive bedrock would produce higher measured EC_a values. However, the depth to bedrock was not known or ascertained, and the EMI survey was not extensive enough to resolve these features.

In Figure 9, Plot B shows the spatial distribution of EC_a across the base of the emptied animal-waste structure. As evident on this plot, EC_a is highest along the southern, and the lower eastern and western edges of the structure's base. The spatial EC_a patterns evident on this plot are associated principally with higher levels of soluble salts from lingering waste residues. A discharge pipe is located on a higher slope area in the southwest corner of the excavated pit (closely outside the survey area). This feature provides additional support for the source of the higher EC_a in the southwest corner of the pit's floor.

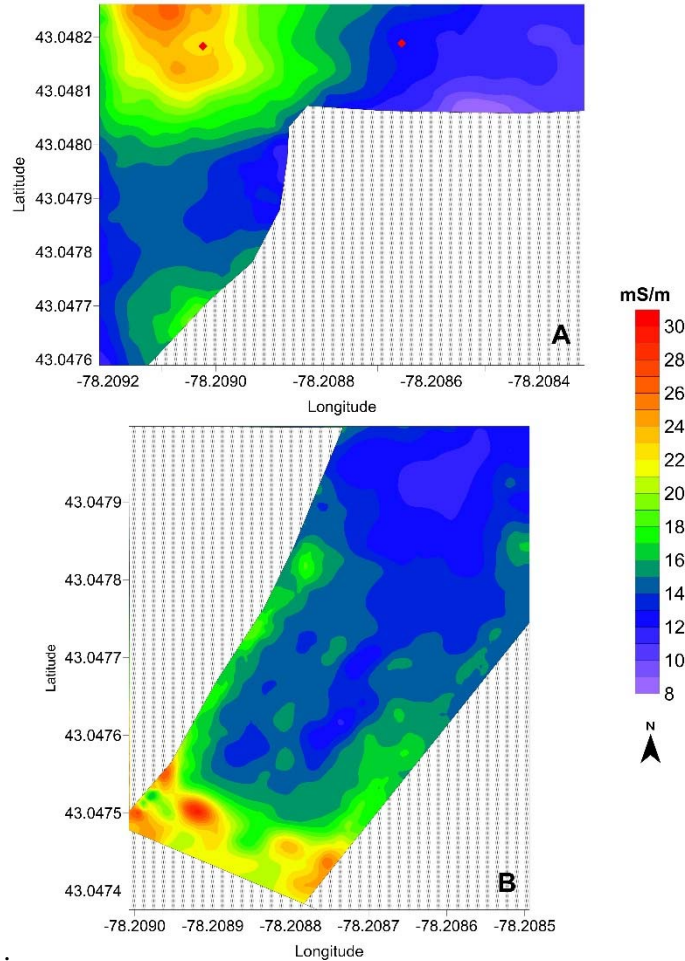


Figure 9. These two-dimensional plot of the EC_a data measured with the EM31 meter were collected across a (A) planned expansion area and (B) an emptied animal-waste storage pit at the Post Farm.

Figure 10 show the spatial distribution of EC_a recorded with the Profiler across the planned storage pit expansion area at frequencies of 15 Hz (upper), 10 Hz (middle), and 5 Hz (lower). In general, EC_a decreases with increasing soil depth (lower frequency), suggesting the presence of more electrically resistive materials with increasing depth. Though unknown at this time, this trend could reflect an increase in rock fragments with depth, presence of coarser textured materials or limestone bedrock within the profiled depths. The spatial EC_a patterns shown on these plots are remarkably similar to one another and to the results obtained with the EM31 meter (Figure 9).

Across the planned expansion area, the averaged EC_a measured with the Profiler decreased with decreasing frequency and increasing depth of exploration. Based on 518 measurements collected with the Profiler, EC_a averaged 25.3, 24.1, and 20.2 mS/m at frequencies of 15, 10 and 5 kHz, respectively. Apparent conductivity measured at 15 kHz ranged from 18.9 to 43.9 mS/m, with one-half of the measurements occurring between 21.4 and 26.2 mS/m. At 10 kHz, EC_a ranged from 17.4 to 43.0 mS/m, with one-half of the measurements occurring between 20.1 and 25.3 mS/m. At 5 kHz, EC_a ranged from 11.7 to 39.2 mS/m, with one-half of the measurements occurring between 16.0 and 21.4 mS/m.

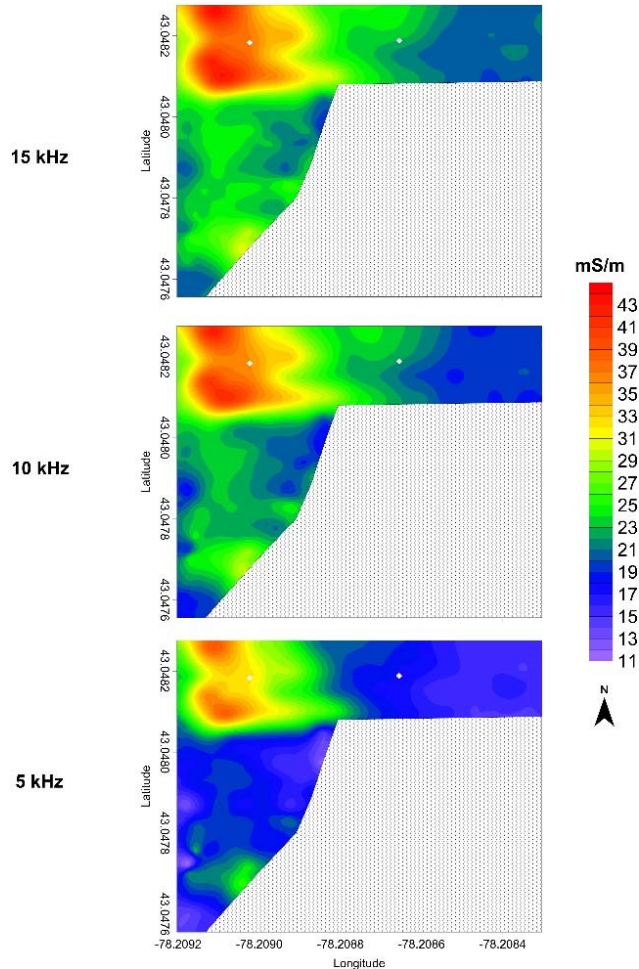


Figure 10. These three, two-dimensional plot of the EC_a data measured with the Profiler sensor at frequencies of 15 (upper plot), 10 (middle plot), and 5 (lower plot) Hz were collected across a planned expansion area for an animal-waste storage pit at the Post Farm.

Across the planned pit expansion area, EMI data measured at different frequencies with the Profiler provided similar EC_a spatial pattern, values, and interpretations. Table 2 shows the correlation among the measurements made at the different frequencies with the Profiler. The EC_a values measured at different frequencies are all highly correlated. While the statistics from this site indicate that EC_a decrease with decreasing frequency and increasing observation depths, these correlations suggest that the use of multiple frequencies provides similar information about this site.

Table 2. Correlations among data sets recorded at different frequencies with the Profiler.

	15 kHz	10 kHz	5 kHz
15 kHz	1.0000	0.9971	0.9894
10 kHz	0.9971	1.0000	0.9934
5 kHz	0.98948	0.9934	1.0000

Figure 11 show the spatial distribution of EC_a recorded with the Profiler across the floor of the existing animal-waste storage pit at frequencies of 15 Hz (upper), 10 Hz (middle), and 5 Hz (lower). In general, EC_a decreases with increasing soil depth (lower frequency). Though not confirmed at this time, this trend could reflect an increase in rock fragments with depth, presence of coarser textured materials or limestone bedrock within the profiled depths. The higher EC_a at shallower depth could reflect the presence of

soluble salts from residual animal wastes. However, spatial EC_a patterns collected with the Profiler (Figure 11) do not appear to mimic those recorded with the EM31 meter (Figure 9).

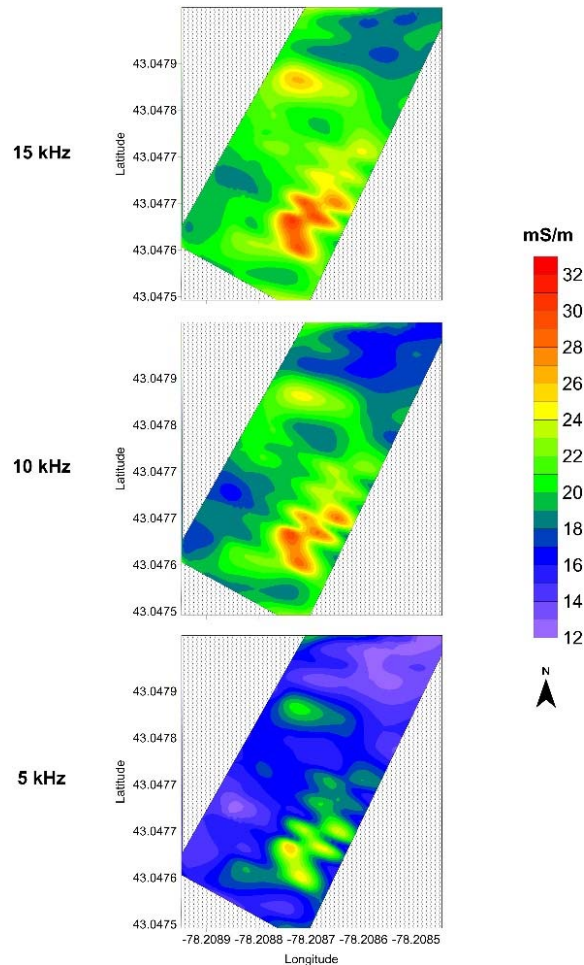


Figure 11. These three, two-dimensional plot of the EC_a data were measured with the Profiler sensor at frequencies of 15 (upper plot), 10 (middle plot), and 5 (lower plot) Hz across the bottom of the existing animal-waste storage pit at the Post Farm.

Based on 407 measurements collected with the Profiler across the bottom of the existing animal-waste storage pit, EC_a averaged 21.2, 20.0, and 16.4 mS/m at frequencies of 15, 10 and 5 kHz, respectively. Apparent conductivity measured at 15 kHz ranged from 17.1 to 30.5 mS/m, with one-half of the measurements occurring between 19.6 and 22.4 mS/m. At 10 kHz, EC_a ranged from 15.7 to 29.8 mS/m, with one-half of the measurements occurring between 17.3 and 21.1 mS/m. At 5 kHz, EC_a ranged from 11.3 to 26.0 mS/m, with one-half of the measurements occurring between 13.6 and 17.6 mS/m. Compared with the measurements collected with the Profiler on the higher-lying pit expansion area, EC_a values were lower and less variable along the floor of the emptied, existing waste-holding pit. The lower values along the waste pit floor may reflect more electrically resistive, coarser-textured materials or bedrock within the profiling depths of the Profiler.

The spatial patterns shown on the three plots in Figure 11 are remarkable similar in form and location. Only the magnitude of the EMI response appears to vary among the three plots with decreasing EC_a values measured at lower frequencies and increasing d_e . Table 3 shows the strong correlation among the measurements made at the different frequencies. The EC_a values measured at different frequencies are all

highly correlated. Once again, EC_a data collected at different frequencies with the Profiler are similar in terms of spatial pattern and interpretations.

Table 3. Correlations among data sets recorded at different frequencies with the Profiler.

	15 kHz	10 kHz	5 kHz
15 kHz	1.0000	0.9971	0.9894
10 kHz	0.9971	1.0000	0.9934
5 kHz	0.9894	0.9934	1.0000

Spatial EC_a patterns manifested in Figures 9, 10, and 11 may provide clues as to the locations of anomalous subsurface conditions, but do not identify solution features. Soil borings and cores are required to confirm interpretations and the presence of solution features.

Offhaus Farms

Radar traverse were conducted across the floor of the newly completed waste-holding facility. This facility had been excavated to limestone bedrock and was covered with a 2 foot “clay” liner. Figure 12 is a representative 2D radar record that was collected with a 400 mHz antenna from this site. On this radar record all scales are expressed in meters. A white-colored, dashed line has been used to highlight the contact of the clay liner with the underlying bedrock. The arrows indicate breaks in the continuity of the bedrock surface. These breaks may represent minor solution features or fractures in the bedrock, but are restricted to the upper part of the bedrock. A green-colored dashed line has been used to indicate a boundary within the overlying clay liner. This may represent a difference in compaction and/or moisture content.

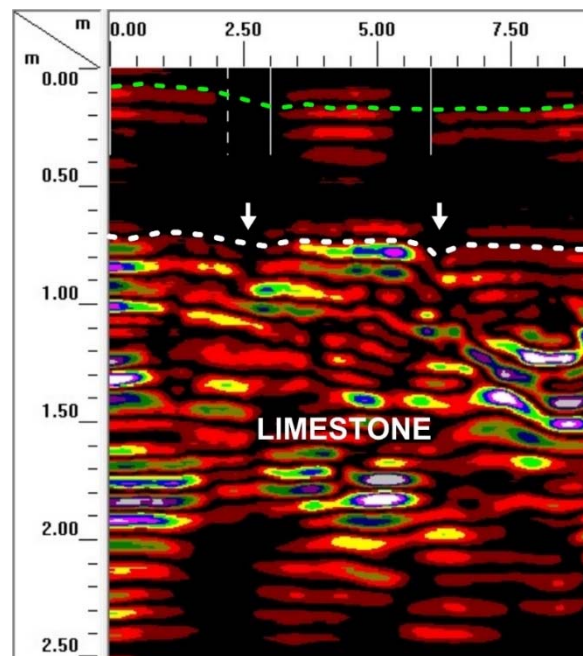


Figure 12. This 2D radar record was collected with a 400 mHz antenna along the floor of the newly completed waste-holding facility at the Offhaus Farms.

Five traverses were completed across the floor of the newly completed waste-holding structure with the 400 mHz antenna. These traverse documented the thickness of the clay liner or the depth to limestone bedrock beneath this structure. Figure 13 shows a 3D image of a radar record collected across this site. On this georeferenced image, the slightly undulating surface of the bedrock is clearly evident as are

several inclined bedding planes within the limestone. These well-expressed bedding planes are more prevalent in the western (left-hand) portion of the radar traverse. Based on 30,338 measurements, the averaged thickness of the clay liner is 0.73 m with a range of 0.29 to 1.20 m along the five GPR traverses. Ninety-five percent of the depth to bedrock measurements are between depths of 0.4 and 1.04 m.

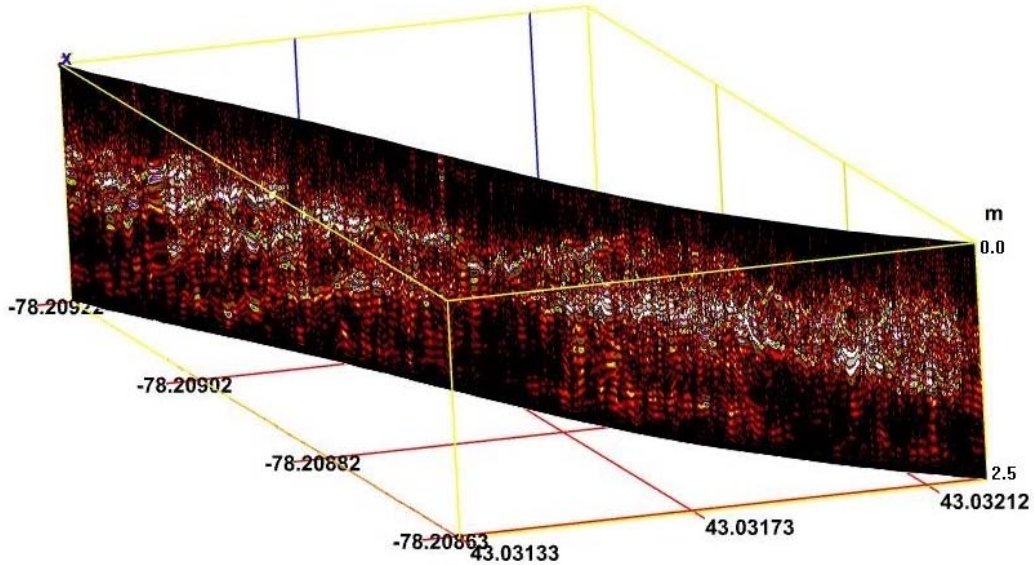


Figure 12. The contact of the clay liner with the underlying limestone bedrock is evident on this 3D rendition of a radar record that was collected with a 400 mHz along the base of the waste-holding facility on the Offhaus Farms

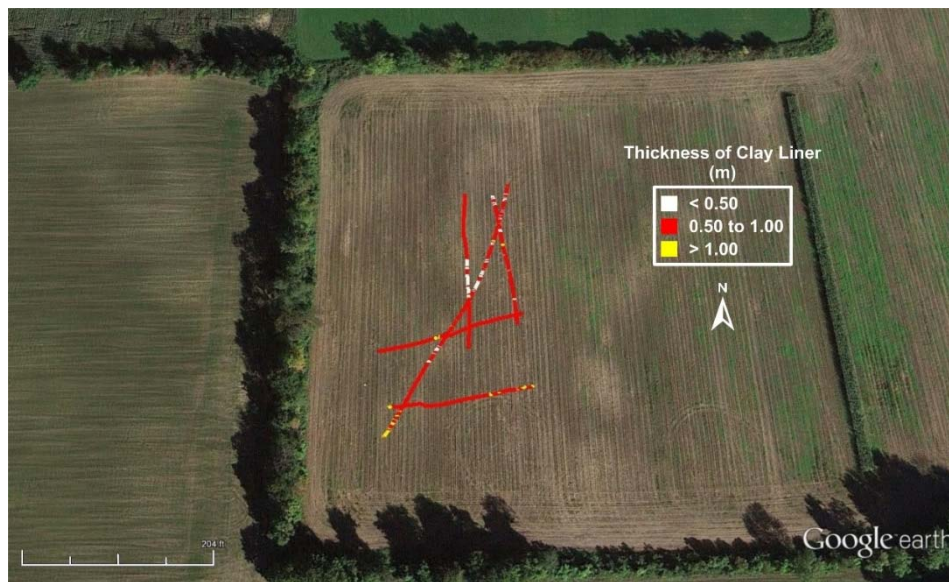


Figure 13. This Google Earth image of the Offhaus Farm site shows the location of five radar traverses that were conducted across the floor of a newly constructed waste-holding structure (not shown). Colors have been used to indicate differences in the thickness of the clay liner.

Figure 14 is a Goggle Earth image of the Offhaus Farm site showing the thickness of the clay liner (or depth to limestone bedrock) along the base of the newly constructed waste-holding facility (not shown). In this image, the locations of the GPR traverse lines are shown. Colors have been used to identify

different soil-depth classes. The clay liner is dominantly moderately deep (50 to 100 cm) with minor areas of shallow (0 to 50 cm) and deep (100 to 150 cm) inclusions.

An EMI survey was conducted across the floor of the newly excavated waste-holding structure with the Profiler. Figure 15 show the spatial distribution of EC_a recorded with the Profiler across this floor at frequencies of 15 Hz (upper), 10 Hz (middle), and 5 Hz (lower). As evident in Figure 15, EC_a increased with increasing soil depth (lower frequency).

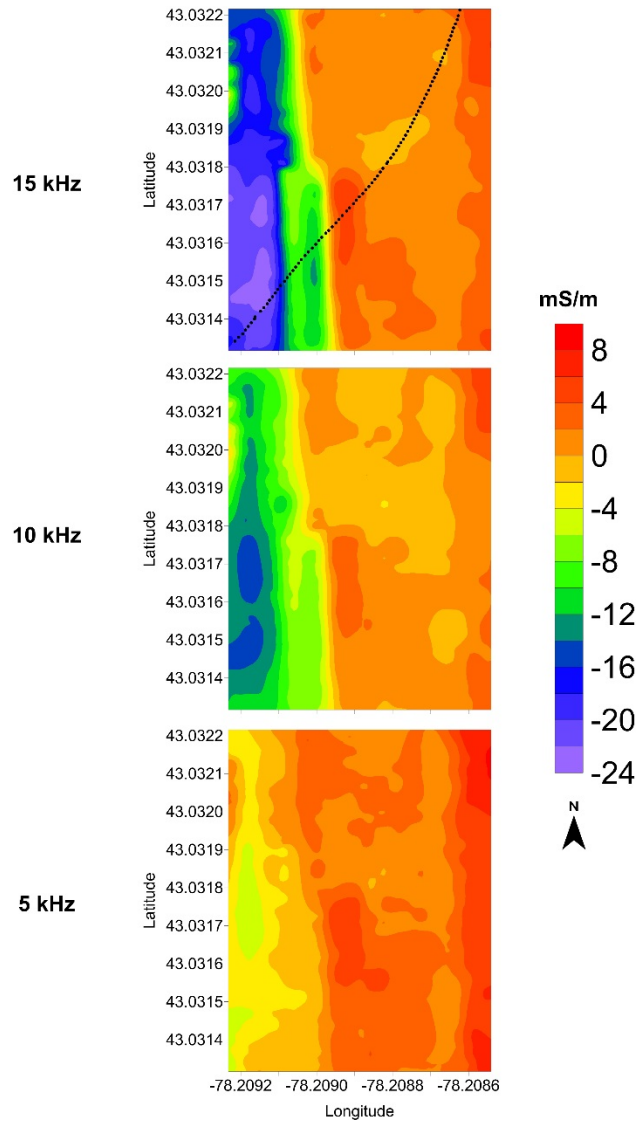


Figure 14. These three, 2D plots of the EC_a data were measured with the Profiler sensor at frequencies of 15 (upper plot), 10 (middle plot), and 5 (lower plot) Hz across the floor of the newly completed waste-holding facility at the Offhaus Farms. The black line in the upper plot shows the location of the radar record shown in Figure 13.

Across the floor of the structure, the averaged EC_a increased with decreasing frequency and increasing depth of exploration. Negative values were unexpectedly and unexplainably recorded in the western 1/3 of the structure. Based on 1591 measurements collected with the Profiler, EC_a averaged -4.773, -3.21, and 1.2 mS/m at frequencies of 15, 10 and 5 kHz, respectively. The low average EC_a can be explained by

the relatively shallow depths to bedrock. The large number and spatially consistent negative values are suspected to be due to variations in lithology and possibly the effects of high levels of magnetic susceptibility. The magnetic susceptibility of earthen materials is largely determined by the presence of iron oxides, in different forms and concentrations. In the upper plot of Figure 15, a black-colored line has been used to identify the location of the radar traverse line shown in Figure 13. The area of negative EC_a values corresponds with the portion of the radar record that shows the most prominent bedding planes in the underlying bedrock.

Across the floor of the newly completed waste-holding facility, EC_a measured at 15 kHz ranged from -22.53 to 4.77 mS/m, with one-half of the measurements occurring between -12.96 and 1.74 mS/m. At 10 kHz, EC_a ranged from -15.16 to 3.96 mS/m, with one-half of the measurements occurring between -7.29 and 0.74 mS/m. At 5 kHz, EC_a ranged from -5.99 to 7.67 mS/m, with one-half of the measurements occurring between -0.74 and 2.97 mS/m.

The spatial patterns shown on the three plots in Figure 15 are similar in general form and location. Only the magnitude of the EMI response appears to vary among the three plots with increasing EC_a values measured at lower frequencies and increasing d_e . Once again, EC_a data collected at different frequencies with the Profiler are similar in terms of spatial pattern and interpretations. Table 4 shows the correlation among the measurements made at the different frequencies. The EC_a values measured at different frequencies are all highly correlated.

Table 4. Correlations among data sets recorded at different frequencies with the Profiler.

	15 kHz	10 kHz	5 kHz
15 kHz	1.0000	0.9884	0.8812
10 kHz	0.9884	1.0000	0.9267
5 kHz	0.8812	0.9267	1.0000

Results of GPR surveys indicates a consistently thick clay liner (average of 0.73 m) and uniform depths to limestone bedrock beneath the recently excavated waste-holding pit at the Offhaus Farms. High resolution GPR surveys indicate the presence of layering, and minor fractures or solution features within the upper portion of the underlying limestone bedrock. Results of EMI surveys conducted with the Profiler do not indicate the presence of major solution features. Results do indicate a major change in the underlying lithology and possibly raised levels of magnetic susceptibility caused by high concentrations of iron oxides.

References:

Brosten, T.R., F.D. Day-Lewis, G.M. Schultz, G.P. Curtis, and J.W. Lane, 2011. Inversion of multifrequency electromagnetic induction data for 3D characterization of hydraulic conductivity. *Journal of Applied Geophysics* 73: 323-335.

Butler, D.K., and J.L. Llopis, 1990. Assessment of anomalous seepage conditions. 153-172 pp. *IN: Ward, S. H. (Ed.) Geotechnical and Environmental Geophysics. Vol. II. Society of Exploration Geophysicists. Tulsa, OK.*

Callegary, J., T.P.A Ferré, and R.W. Groom, 2007. Vertical spatial sensitivity and exploration depth of low-induction-number electromagnetic-induction instruments. *Vadose Zone Journal* 6: 158-167.

Canace, R., and R. Dalton, 1984. A geological survey's cooperative approach to analyzing and remedying a sinkhole related disaster in an urban environment. pp. 342-348. *IN: Proceedings of the First Multidisciplinary Conference on Sinkholes. Orlando, Florida. 15 to 17 October 1984.*

Cassidy, N.J. 2009. Electrical and magnetic properties of rocks, soils, and fluids. In *Ground Penetrating Radar: Theory and Applications*, ed. H. M. Jol, 41-72 pp. Elsevier Science, Amsterdam, The Netherlands.

Daniels, D. J., 2004. *Ground Penetrating Radar*; 2nd Edition. The Institute of Electrical Engineers, London, United Kingdom.

de Jong, E., A.K. Ballantyne, D.R. Cameron, and D.L. Read, 1979. Measurement of apparent electrical conductivity of soils by an electromagnetic induction probe to aid salinity surveys. *Soil Science Society of America Journal* 43:810-812.

Dominic, D. F., K. Egan, C. Carney, P. J. Wolfe, and M. R. Boardman, 1995. Delineation of shallow stratigraphy using ground penetrating radar. *Journal of Applied Geophysics* 33: 167-175.

Geophysical Survey Systems, Inc., 2004. TerraSIRch SIR System-3000; User's Manual. MN72-433 Rev D. Geophysical Survey Systems, Inc., North Salem, New Hampshire, USA.

Geophysical Survey Systems, Inc., 2008. Profiler EMP-400. User's Manual. Geophysical Survey Systems, Inc., North Salem, New Hampshire, USA.

Greenhouse, J.P., and D.D. Slaine, 1983. The use of reconnaissance electromagnetic methods to map contaminant migration. *Ground Water Monitoring Review* 3(2): 47-59.

Greenhouse, J.P., D.D. Slaine, and P. Gudjurgis, 1998. Application of geophysics in environmental investigations. Matrix Multimedia, Canada. CD-ROM.

Huang, H., 2005. Depth of investigation for small broadband electromagnetic sensors. *Geophysics*, 70 (6): G135–G142.

Kachanoski, R.G., E.G. Gregorich, and I.J. Van Wesenbeeck, 1988. Estimating spatial variations of soil water content using noncontacting electromagnetic inductive methods. *Canadian Journal of Soil Science* 68:715-722.

Karastathis, V.K., P.N. Karmas, G. Dramatis, and G. Stavrakakis, 2002. Geophysical methods contributing to the testing of concrete dams. Application at the Marathon Dam. *Journal of Applied Geophysics* 50: 247-260.

McNeill, J.D., 1980a. Electrical Conductivity of soils and rocks. Technical Note TN-5. Geonics Ltd., Mississauga, Ontario.

McNeill, J.D., 1980b. Electromagnetic terrain conductivity measurement at low induction numbers. Technical Note TN-6. Geonics Limited, Mississauga, Ontario.

McNeill, J.D., 1996. Why doesn't Geonics Limited Build a Multi-frequency EM31 or EM38? Technical Note TN-30. Geonics Limited, Ontario, Canada.

Jol, H., 2009. *Ground Penetrating Radar: Theory and Applications*. Elsevier Science, Amsterdam, The Netherlands.

Pazuniak, B.L., 1989. Subsurface investigation response to sinkhole activity at an eastern Pennsylvania site. pp. 263-269. IN: *Proceedings of the 3rd Multidisciplinary Conference on Sinkholes*. St. Petersburg Beach, Florida. 2 to 4 October 1989.

- Rhim, H.C., 2001. Condition monitoring of deteriorating concrete dams using radar. *Cement and Concrete Research* 31: 363- 373.
- Rhoades, J.D., P.A. Raats, and R.J. Prather, 1976. Effects of liquid-phase electrical conductivity, water content, and surface conductivity on bulk soil electrical conductivity. *Soil Science Society of America Journal* 40:651-655.
- Robinson-Poteet, D., 1989. Using terrain conductivity to detect subsurface voids and caves in a limestone formation. pp. 271-279. IN: Proceedings of the 3rd Multidisciplinary Conference on Sinkholes. St. Petersburg Beach, Florida. 2 to 4 October 1989.
- Rumbens, A.J., 1990. Detection of cavities in karstic terrain: road subsidence - Snowy Mountains Highway near Yarrangobilly, State of new South Wales - Australia. *Exploration Geophysics* 21:121-24.
- Saksa, P., and J. Sorsa (In press). System stability and calibration for hand-held electromagnetic frequency domain instruments. *Near Surface Geophysics*.
- Silver, M.L., P.S. Fisk, and A. Greenman, 1986. Grouting a sand dam. *Civil Engineering*. December 1986.
- Slavich, P.G., 1990. Determining EC"-depth profiles from electromagnetic induction measurements. *Australian Journal Soil Research*. 28:443-452.
- Won, I.J., 1980. A wideband electromagnetic exploration method - Some theoretical and experimental results. *Geophysics* 45: 928-940
- Won, I.J., 1983. A sweep-frequency electromagnetic exploration method. 39-64 pp. IN: A.A. Fitch (editor) *Development of Geophysical Exploration Methods*. Elsevier Applied Science Publishers, Ltd. London.
- Won, I.J., D.A. Keiswetter, G.R.A. Fields, and L.C. Sutton, 1996. GEM-2; Anew multifrequency electromagnetic sensor. *Journal of Environmental & Engineering Geophysics* 1:129-137.